DETERMINATION OF TENSION FOR ARAMID AND CARBON YARNS WHILE WEAVING INDUSTRIAL FABRICS

Volodymyr Shcherban'[1], Oksana Kolysko[1], Gennadiy Melnyk[1], Marijna Kolysko[1], Yuriiy Shcherban'[2] and Ganna Shchutska[2]

[1]Kyiv National University of Technologies and Design, Nemirovicha-Danchenko str. 2, 01011 Kyiv, Ukraine
[2]Department of Light Industry Technologies State Higher Educational Establishment «Kyiv College of Light Industry» Ivana Kudri str. 29, 01601 Kyiv, Ukraine
melnik2000@ukr.net

Abstract: *Resulting from researches conducted to determine tension for para-aramid, meta-aramid, and carbon multifilament yarns during their contact with the operative parts of the weaving looms as part of the industrial fabrics formation process, we have found out that in threading areas the tension is increasing driven by variation of values of the friction forces in the contact area. It has been proven that tension degree of para-aramid, meta-aramid, and carbon multifilament yarns before industrial fabric formation area is influenced by (1) tension before cylindrical guide surface of an operative part, (2) radius of the cylindrical guide surface curve of the operative part, (3) contact angle between yarns and cylindrical guide surface of an operative part, (4) mechanical, physical and structural properties of para-aramid, meta-aramid, and carbon multifilament yarns. It allowed (yet at the initial stage of design of technological process of industrial fabric formation) to determine para-aramid, meta-aramid, and carbon multifilament yarns tension before formation area depending on (1) form of threading line for yarns at the weaving loom, (2) mechanical, physical and structural properties of para-aramid, meta-aramid, and carbon multifilament yarns and industrial fabrics. The paper contains experimental research of interaction of para-aramid, meta-aramid, and carbon multifilament yarns and cylindrical guide surfaces of the operative parts of automatic weaving looms. Based on experimental researches regression dependencies have been obtained between para-aramid, meta-aramid, and carbon multifilament yarns tension value after cylindrical guide surfaces of the operative part and (1) tension before cylindrical guide surface of the operative part, (2) radius of the cylindrical guide surface curve of the operative part, (3) contact angle between yarns and cylindrical guide surface of the operative part. Consecutive application of these regression dependencies allows to determine para-aramid, meta-aramid, and carbon multifilament yarns tension before industrial fabrics formation area. Analysis of regression dependencies allowed to find out values of technological parameters when para-aramid, meta-aramid, and carbon multifilament yarns tension before industrial fabrics formation area will be of minimum value. It will allow to minimize tension of para-aramid, meta-aramid, and carbon multifilament yarns while manufacturing resulting in (1) yarn breakages reduction, (2) better productivity of weaving looms due to reduced stoppage time, (3) improved quality of manufactured industrial fabrics. Therefore, we can argue that suggested technological solutions are practically attractive. In view of this, it is reasonable to say that it is possible to directionally regulate the process of para-aramid, meta-aramid, and carbon multifilament yarns tension change while manufacturing industrial fabrics on the weaving looms through selection of values of guides' geometrical parameters.*

Keywords: *industrial fabrics, para-aramid multifilament yarns, meta-aramid multifilament yarns, carbon multifilament yarns, tension, contact angle, guide's curve radius.*

1 INTRODUCTION

Yarns tension on the weaving looms and knitting machines [1-3] is a determining factor for evaluation of the density of fabric and knit formation process. The papers [4-7] show that tension of polyethylene, polyamide, and basalt multifilament yarns consists of the threading tension and additional tension arising due to frictional forces between yarns and surfaces of guides and operative parts of the weaving loom which have cylindrical form or one close to it. The value of friction forces depends on the material of yarn and guide [2], curve of guides surfaces and operative parts of the weaving looms and knitting machines [4, 6], actual contact angle between the yarn and cylindrical guide of the operative part [2, 3, 5-6], mechanical, physical and structural properties of the multifilament yarns, as well as tension before the guide [1, 7].

Simulation of the warp yarns manufacturing process at the weaving loom involves research of the process of interaction between warp yarns and cylindrical guides of the operative parts which imitate surfaces of back rest [8-14], separating rod of yarn break detector, heddle eyes of heald frame for automatic [12], shuttleless looms when manufacturing single-layer and multilayer fabrics [8, 10].

When a yarn passes all guides consecutively, from the input area to the area of fabric formation, it leads to step-type increase in tension [14]. Output parameter of tension after the previous guide will be equal to input parameter for the following guide, which allows to use recursion to determine tension before single-layer and multilayer fabrics formation area [6, 8, 9, 14]. That sort of interaction occurs during similar technological processes [15, 16].

Simulation of warp yarns manufacturing process at the weaving loom involves research of the interaction process between warp yarns and cylindrical surfaces imitating the surfaces of the back rest, the separating rod of yarn break detector, heddle eyes of heald frame for automatic shuttleless pneumatic rapier looms [4, 5, 8]. Increase in measuring accuracy of para-aramid, meta-aramid, and carbon multifilament yarns tension and possibility to ensure metrological self-control are facilitated by use of redundant measurements method. This method ensures independence of measurement result from parameters of conversion function and their deviations from nominal values [17-19]. While planning the experiment it is necessary to consider direction of relative shifting of friction surface [20, 21], yarn sliding speed or guide surface movement speed [22, 24], curvature radius of cylindrical surface [17, 18, 25]. Taking into account that para-aramid, meta-aramid, and carbon multifilament yarns are used as warp yarns bending rigidity can be ignored [2, 13].

To carry out experimental researches aimed at determining para-aramid, meta-aramid, and carbon multifilament yarns tension after the guide's surface the special strain-gauge unit is to be designed. The paper [7] emphasizes the necessity to consider that if the value of multifilament yarns throwing greater the value of its bending rigidity will also be greater. Bending rigidity significantly influences the value of the actual contact angle between the yarn and the guide's surface. It was confirmed in papers [4, 5] while carrying out research of conditions of interaction between polyethylene, polyamide, and basalt multifilament yarns and guide's surface.

Results of experimentally determined (with the help of special units) tension of multifilament yarns were provided in the papers [4-6, 8-14].

Design of the experimental unit estimates the accuracy of the obtained results, while determining yarn tension. The papers [23-24] show the scheme for determination of the yarn tension. In this scheme the cylinders with big radii are used as guides. Among its drawbacks is impossibility to simulate real conditions of interaction between the yarn and guide and operative parts of looms with large curvature. The same drawbacks come with experimental unit with revolving cylinder [25].

2 MATERIALS

Industrial fabrics from aramid and carbon multifilament yarns are widely used in different industry fields (Figure 1). It can be explained by their unique physical and mechanical properties. Aramid fabrics are used to manufacture overalls for military men, lifeguards, firemen, metallurgists. They are also used to produce clothes, battle dress uniform, bullet-proof vests, helmets, harness. Aramid fabrics are highly resistant to mechanical stress and able to hold its shape during the whole period of usage. Strength of aramid fabrics is greater than steel strength. The weight of aramid fabrics is small. They are weighing less than fiberglass materials and are able to retain protective properties at very high temperatures.

All aramid fibers have extra thermal protection. Meta-aramid fabrics (Figure 1a) are extra strong. Para-aramid fabrics (Figure 1b) provide extra protective properties.

Carbon fabrics (Figure 1c) is the basis in manufacture of carbon fiber reinforced plastic and all-carbon composites. They are used in chemical industry, oil refining industry, metallurgic industry, pulp-and-paper industry and other industry fields. They are suitable for insulation, heating elements, gas filters, liquids and melts, as well as for encapsulation of different compounds. They also may be used as current consuming elements and electrodes for electrochemical processes, as well as fiber fillers to produce chemically stable composites with polymer and carbon matrixes. This material is heat-resistant, electrically conductive, multifunctional, and resistant to corrosive environment.

Figure 1 Industrial fabrics: a) Kevlar from para-aramid multifilament yarns 44 tex; b) Nomex from meta-aramid multifilament yarns 40 tex; c) fabric from carbon multifilament yarns 30 tex

Para-aramid and meta-aramid multifilament yarns were chosen as warp yarns to manufacture technical aramid fabrics. Carbon multifilament yarns were chosen for carbon technical fabrics. To conduct the experiment, the following yarns were taken: extra strong para-aramid multifilament yarns 44 tex (Figure 2a); meta-aramid multifilament yarns 40 tex providing extra thermal protection (Figure 2b); carbon yarns H-30 with thickness 30 tex (Figure 2c). They are used to produce insulation, heating units, gas filters, liquids and melts, as well as encapsulation of different compounds. We have chosen aramid and carbon yarns of approximately the same thickness. To determine diameters of the chosen yarns we used Sigeta USB digital microscope expert (magnification 10x-300x) (Figure 2d).

Figure 2 Yarns for experiment: a) para-aramid multifilament yarn 44 tex; b) meta-aramid multifilament yarn 40 tex; c) carbon yarn H-30 with thickness 30 tex; d) Sigeta USB digital microscope expert (magnification 10x-300x)

3 EXPERIMENT

Three types of multifilament yarns were chosen to conduct the experiment. Series PA: para-aramid multifilament yarns 44 tex. They used as warp yarns to produce extra strong fabrics, and then used to sew workwear, military apparel. They may be added to the makeup of composite materials and used for reinforcement of cable products. Series MA: meta-aramid multifilament yarns 40 tex. They are used as warp yarns to produce overalls for metallurgy, firefighting, welding, and fabrics suitable for canvas top for vehicles transporting asphalt and other high temperature cargos. Series CA: carbon multifilament yarns 30 tex. They are used as warp yarns to produce insulation, heating units, gas filters, liquids and melts, as well as encapsulations of different compounds.

For each series PA, MA and CA to determine joint influence between slack side tension of warp yarn P_0, radius of cylindrical guide R, nominal value of contact angle φ_P and tight side tension of warp yarn P in the paper has been planned and implemented second order orthogonal design for three factors [8-14]. General form of regression equation is as follows:

$$P = b_0 + b_1x_1 + b_2x_2 + b_3x_3 + b_{12}x_1x_2 + \\ +b_{13}x_1x_3 + b_{23}x_2x_3 + +b_{11}x_1^2 + b_{22}x_2^2 + b_{33}x_3^2 \quad (1)$$

Range of factors variations in equation (1) is determined by actual conditions of manufacturing of para-aramid, meta-aramid, and carbon multifilament yarns at the weaving looms. Threading line of warp yarns is divided into three areas: I - area from point of warp yarn coming off the beam up to the dropper mechanism; II – area of warp yarn entry to the dropper mechanism up to the heald frame; III – area from warp yarn exit from dropper mechanism up to the fell of the fabric (Figure 3a, 3b). In the I area para-amid, meta-aramid, and carbon multifilament yarns contact with back rest. In the II area para-amid, meta-aramid, and carbon multifilament yarns contact with dropper separating mechanism. In the III area para-amid, meta-aramid, and carbon multifilament yarns contact with heddle eyes of heald frame.

As a result of the implementation of the experimental plans for each series of PA, MA and SA and for each zone I, II and III, were taken 10 analytical measurements for 30 threads. For this experimental unit guide rollers with a working surface of 60 mm are used. The average tension values were taken for different moments of formation of fabric elements on looms.

The influence of the beating of the weft thread and shed formation on the deformation of para-aramid, meta-aramid and carbon complex threads was taken into account by selecting the value of the input tension in the cell.

Factor x_1 is a value of threading tension in the I area and up to back rest for weaving looms (Figure 3a, 3b). Depending on the type of warp yarns: PA - for para-aramid multifilament yarns P_{0I} = 38 cN; MA - for meta-aramid multifilament yarns P_{0I} = 26 cN; CA - for carbon multifilament yarns P_{0I} = 32 cN.

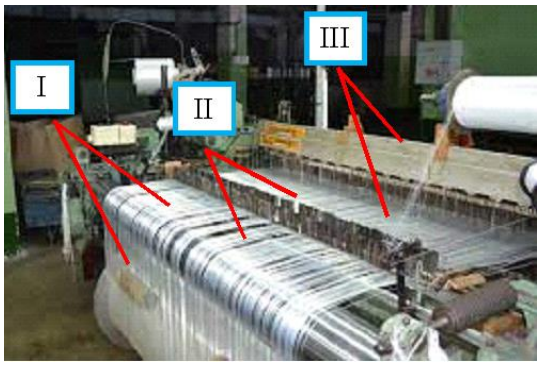

a)

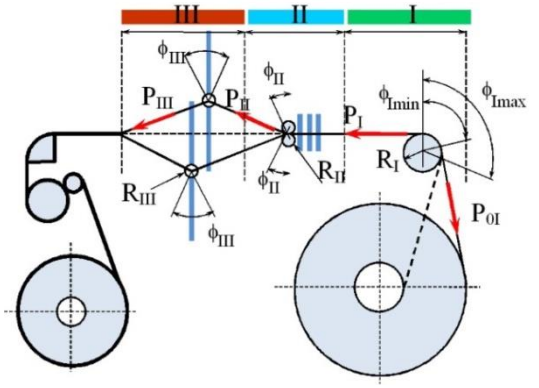

b)

Figure 3 Weaving loom: a) warp yarns threading areas of the weaving loom; b) warp yarn threading scheme at the weaving loom

Factor x_2 - a cylinder radius (imitating back rest surface) in the I area, and for different looms it ranges from R_I = 63 mm to R_I = 32 mm. Factor x_2 - a cylinder radius (imitating surface of the left separating rod in the dropper mechanism) in the II area, for different looms it ranges from R_{II} = 9 mm to R_{II} = 3 mm. Factor x_2 - a cylinder radius (imitating surface of heddle eyes of heald frame) in the III area, for different looms it ranges from R_{III} = 1.1 mm to R_{III} = 0.5 mm.

Factor x_3 - nominal value of the contact angle between the yarn and the cylinder (imitating back rest surface) in the I area, and for different looms it ranges from φ_{IP} = 110° at maximum diameter of the beam to φ_{IP} = 90° at minimum diameter of the beam. Factor x_3 - nominal value of the contact angle between the yarn and the cylinder (imitating surface of the left separating rod in the dropper mechanism) in the II area, and for different looms it ranges from φ_{IIP} = 76° when shed is opened for maximum to φ_{IIP} = 0° when shed is closed. Factor x_3 - nominal value of the contact angle between the yarn and the cylinder (imitating surface of heddle eyes of heald frame) in the III area, and for different looms it ranges from φ_{IIIP} = 41° with open shed to φ_{IIIP} = 0° with closed shed.

At the first stage we determine tension in the I area after the beck rest. Table 1 shows matrix of second-order orthogonal design for three series PA, MA and CA.

Table 1 Matrix of second-order orthogonal design for three series PA, MA and CA for the I area

№	Factors					
	Input tension		Curvature radius		Contact angle	
	x_1	P_{0I} [cN]	x_2	R_I [mm]	x_3	φ_{IP} [°]
1	+1	48	36	42	+1	65
2	-1	28	16	22	+1	65
3	+1	48	36	42	-1	35
4	-1	28	16	22	-1	35
5	+1	48	36	42	+1	65
6	-1	28	16	22	+1	65
7	+1	48	36	42	-1	35
8	-1	28	16	22	-1	35
9	-1.215	26	14	20	0	50
10	+1.215	50	38	44	0	50
11	0	38	26	32	-1.215	32
12	0	38	26	32	+1.215	68
13	0	38	26	32	0	50
14	0	38	26	32	0	50
15	0	38	26	32	0	50

Connection between denominated and coded values of the I area for para-amid, meta-aramid, and carbon multifilament yarns is as follows:

series PA

$$x_1 = \frac{P_{0I} - 38}{10}, x_2 = \frac{R_I - 50}{15}, x_3 = \frac{\varphi_{IP} - 110}{10} \quad (2)$$

series MA

$$x_1 = \frac{P_{0I} - 26}{10}, x_2 = \frac{R_I - 50}{15}, x_3 = \frac{\varphi_{IP} - 110}{10} \quad (3)$$

series CA

$$x_1 = \frac{P_{0I} - 32}{10}, x_2 = \frac{R_I - 50}{15}, x_3 = \frac{\varphi_{IP} - 110}{10} \quad (4)$$

At the second stage we determine tension in the II area after the left separating rod in the dropper mechanism. As an input tension P_{0II} we take output tension of para-amid, meta-aramid, and carbon multifilament yarns after the I area P_I. Table 2 shows matrix of second-order orthogonal design for three series PA, MA and CA.

Table 2 Matrix of second-order orthogonal design for three series PA, MA and CA for the II area

№	Factors					
	Input tension		Curvature radius		Contact angle	
	x_1	P_{0II} [cN]	x_2	R_{II} [mm]	x_3	φ_{IIP} [°]
1	60	48	52	+1	8	+1
2	36	20	28	+1	8	+1
3	60	48	52	-1	2	+1
4	36	20	28	-1	2	+1
5	60	48	52	+1	8	-1
6	36	20	28	+1	8	-1
7	60	48	52	-1	2	-1
8	36	20	28	-1	2	-1
9	33	17	25	0	5	0
10	63	51	55	0	5	0
11	48	34	40	-1.215	1	0
12	48	34	40	+1.215	9	0
13	48	34	40	0	5	-1.215
14	48	34	40	0	5	+1.215
15	48	34	40	0	5	0

Connection between denominated and coded values of the II area for para-amid, meta-aramid, and carbon multifilament yarns is as follows:

series PA

$$x_1 = \frac{P_{0II} - 48}{12}, x_2 = \frac{R_{II} - 5}{3}, x_3 = \frac{\varphi_{IIP} - 45}{35} \quad (5)$$

series MA

$$x_1 = \frac{P_{0II} - 34}{14}, x_2 = \frac{R_{II} - 5}{3}, x_3 = \frac{\varphi_{IIP} - 45}{35} \quad (6)$$

series CA

$$x_1 = \frac{P_{0II} - 40}{12}, x_2 = \frac{R_I I - 5}{3}, x_3 = \frac{\varphi_{IIP} - 45}{35} \quad (7)$$

At the third stage we determine tension in the III area after the heddle eyes of heald frame. As an input tension P_{0III} we take output tension of para-amid, meta-aramid, and carbon multifilament yarns after the II area P_{0II}. Table 3 shows matrix of second-order orthogonal design for three series PA, MA and CA.

Table 3 Matrix of second-order orthogonal design for three series PA, MA and CA for the III area

№	Factors					
	Input tension		Curvature radius		Contact angle	
	x_1	P_{0III} [cN]	x_2	R_{III} [mm]	x_3	φ_{IIIP} [°]
1	+1	70	58	64	+1	1.4
2	-1	42	26	32	+1	1.4
3	+1	70	58	64	-1	0.6
4	-1	42	26	32	-1	0.6
5	+1	70	58	64	+1	1.4
6	-1	42	26	32	+1	1.4
7	+1	70	58	64	-1	0.6
8	-1	42	26	32	-1	0.6
9	-1.215	39	23	29	0	1
10	+1.215	73	61	67	0	1
11	0	56	42	48	-1.215	0.5
12	0	56	42	48	+1.215	1.5
13	0	56	42	48	0	1
14	0	56	42	48	0	1
15	0	56	42	48	0	1

Connection between denominated and coded values of the III area for para-amid, meta-aramid, and carbon multifilament yarns is as follows:

series PA

$$x_1 = \frac{P_{0III} - 56}{14}, x_2 = \frac{R_{III} - 1}{0.4}, x_3 = \frac{\varphi_{IIIP} - 22}{18} \quad (8)$$

series MA

$$x_1 = \frac{P_{0III} - 42}{16}, x_2 = \frac{R_{III} - 1}{0.4}, x_3 = \frac{\varphi_{IIIP} - 22}{18} \quad (9)$$

series CA

$$x_1 = \frac{P_{0III} - 48}{16}, x_2 = \frac{R_{III} - 1}{0.4}, x_3 = \frac{\varphi_{IIIP} - 22}{18} \quad (10)$$

Figure 4a) shows principal scheme of the experimental unit. The first unit 1 is one for supply and tensioning of para-amid, meta-aramid, and carbon multifilament yarns. Input tension was created using tensioner. The second 2 and the third 3 units are designed for metering tension of slack side and tight side of the para-amid, meta-aramid, and carbon multifilament yarns 9. They have two rollers, which are installed in the bearings on the stationary axles. The third roller is installed on the cantilever fitted beam in a way that inner ring of the bearing fixed on it, and the roller which contacts with para-amid, meta-aramid, and carbon multifilament yarns is rigidly fixed with outer ring of the bearing. Friction forces in bearings we can ignore. Warp yarn were threaded into pulley in a way that slack and tight sides were places by both sides of right triangle.

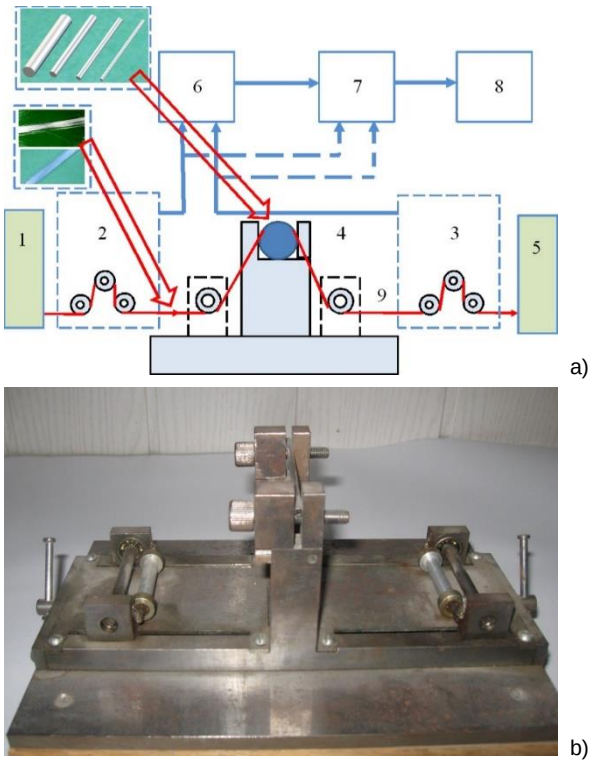

Figure 4 Scheme of the experimental unit: a) principal scheme: 1 - the yarn threading unit; 2 - metering unit for slack side tension of the yarn; 3 - metering unit for tight side tension of the yarn; 4 - unit for simulation of interaction conditions between the yarn and guides and operative parts of the textile machinery; 5 - yarn receiving unit; 6 - amplifier; 7 - analogue-to-digital converter ADC; 8 - PC; 9 - the yarn; b) central metering unit

Affected by para-amid, meta-aramid, and carbon multifilament yarns tension central bar has been bending, which has resulted in variations in resistance of strain-gauge indicator. These variations have been registered at the corresponding channel of the amplifier 8ANCH-7M. Lateral and longitudinal dimensions of the beam have been chosen such that free-running frequency of the beam has been 1400 Hz. This frequency goes beyond frequency of the highest tension component way more. Figure 4b) represents central metering unit 4 of the experimental unit. This metering unit

is intended for simulation of interaction conditions between the para-amid, meta-aramid, and carbon multifilament yarns 9 and cylindrical guides. Two slider pairs, on which aluminium rollers are fixed in rotation bearings, are installed on the foundation in the horizontal grooves. The position of the slider pairs with respect to the central fixed bracket is changed with the help of two screw pairs by turning the two levers on the left and on the right. The central, fixed vertical bracket serves to secure the cylinder guides of different diameters, needles of knitting machine, heddles. The fastening is carried out by two screw pairs and clamping bars.

The para-amid, meta-aramid, and carbon multifilament yarns 9 speed was varied due to a fixed ratio round belt transmission – unit 5 (Figure 4a). Driving pulley of the transmission is rotated by AC motor that was firmly fixed to the foundation of the main measurement system. Analogue signals from the 3rd and 4th units measuring yarn tension is being received by the amplifier 6 or by analogue-to-digital converter 7, enabled as a multifunction board L-780M with signalling processor ADC 14 bit/400 kHz having 16 differential input analogue and output digital channels, which is connected to the PCI-connector of the PC 8.

4 RESULTS AND DISCUSSION

As a result of implementation of designs of the experiment (Tables 1-3) for each series PA, MA and CA and for each area I, II and III the 10 parallel measurements have been conducted, and their average values are represented in Table 4.

Using known method for determining coefficients in regression equation (1) for second order orthogonal design [8-14], considering dependencies (2-10), the following regression dependencies have been obtained:

For the I area:

series PA - para-aramid multifilament yarn 44 tex

$$P_I = 3.22 + 0.93P_{0I} - 0.008R_I - 0.036\varphi_{PI} + \\ +0.00013P_{0I}R_I + 0.0033P_{0I}\varphi_{PI} + 0.00008R_I\varphi_{PI} - \\ -0.00009P_{0I}^2 - 0.00003R_I^2 + 0.00015\varphi_{PI}^2, \quad (11)$$

series MA - meta-aramid multifilament yarn 40 tex

$$P_I = 1.29 + 0.96P_{0I} - 0.003R_I - 0.009\varphi_{PI} + \\ +0.00008P_{0I}R_I + 0.0021P_{0I}\varphi_{PI} + 0.00003R_I\varphi_{PI} - \\ -0.0001P_{0I}^2 - 0.000002R_I^2 + 0.00004\varphi_{PI}^2, \quad (12)$$

series CA - carbon yarn H-30 with thickness 30 tex

$$P_I = 1.90 + 0.94P_{0I} - 0.005R_I - 0.017\varphi_{PI} + \\ +0.0001P_{0I}R_I + 0.0027P_{0I}\varphi_{PI} + 0.00002R_I\varphi_{PI} - \\ -0.00014P_{0I}^2 - 0.00002R_I^2 + 0.00007\varphi_{PI}^2. \quad (13)$$

Table 4 Results of tension determination for each series PA, MA and CA and for each area: I, II and III

Exp №	Warp yarn output tension *Pi*, cN								
	Para-aramid multifilament yarn 44 tex			Meta-aramid multifilament yarn 40 tex			Carbon yarn H-30 with thickness 30 tex		
	i=I	*i*=II	*i*=III	*i*=I	*i*=II	*i*=III	*i*=I	*i*=II	*i*=III
1	65.44	73.85	83.21	44.72	55.48	65.30	54.78	62.02	73.44
2	38.36	44.44	50.03	19.98	23.19	29.34	28.84	33.50	36.79
3	65.21	76.84	93.87	44.61	56.97	70.85	54.59	63.81	80.15
4	38.22	46.26	56.50	19.93	23.83	31.87	28.74	34.47	40.18
5	62.16	62.26	76.05	43.14	49.24	61.34	52.41	53.58	68.01
6	36.41	37.37	45.67	19.26	20.53	27.52	27.57	28.86	34.08
7	61.99	64.68	85.18	43.06	50.52	66.22	52.28	55.06	73.76
8	36.31	38.84	51.19	19.22	21.07	29.74	27.49	29.66	36.92
9	34.67	37.64	45.90	17.16	18.64	25.72	25.61	27.91	32.85
10	66.32	71.69	85.74	46.30	55.79	68.06	56.04	61.27	75.76
11	50.41	59.91	74.99	31.70	39.59	51.24	40.77	47.64	59.66
12	50.60	54.22	63.35	31.79	37.02	45.69	40.91	44.34	52.83
13	48.98	49.33	62.20	31.07	34.64	45.08	39.78	40.83	51.74
14	52.09	60.74	69.66	32.44	40.07	48.79	41.94	48.81	57.01
15	50.51	54.68	65.83	31.75	37.23	46.89	40.85	44.59	54.32

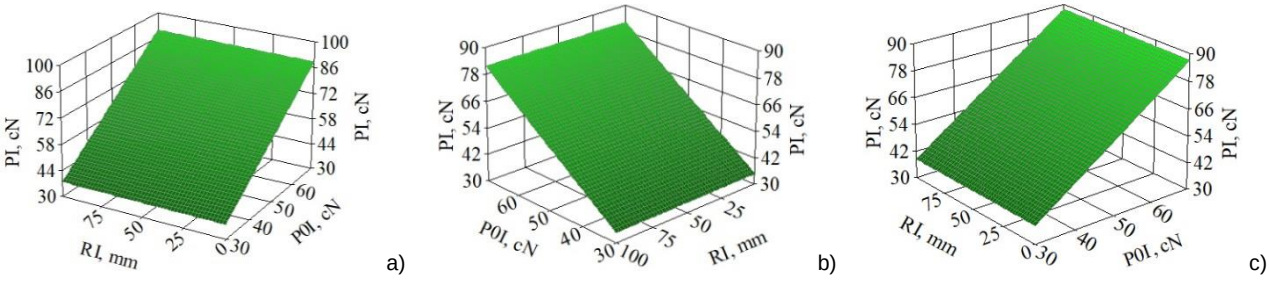

Figure 5 Graphical dependencies of the warp yarns tension for the I area of the weaving loom: a) - para-aramid multifilament yarn; b) - meta-aramid multifilament yarn; c) - carbon yarn H-30

Adequacy of obtained regression dependencies has been verified with SPSS program for statistical processing of experimental data [8-14].

For the II area:

series PA - para-aramid multifilament yarn 44 tex

$$P_{II} = -1.72 + 1.27P_{0II} - 1.31R_{II} + 0.014\varphi_{PII} - \\ -0.007P_{0II}R_{II} + 0.0027P_{0II}\varphi_{PII} - 0.0011R_{II}\varphi_{PII} - \\ -0.0023P_{0II}^2 + 0.12R_{II}^2 - 0.00008\varphi_{PII}^2, \quad (14)$$

series MA - meta-aramid multifilament yarn 40 tex

$$P_{II} = -5.32 + 0.65P_{0II} - 0.20R_{II} + 0.15\varphi_{PII} - \\ -0.001P_{0II}R_{II} + 0.009P_{0II}\varphi_{PII} - 0.0003R_{II}\varphi_{PII} - \\ -0.0025P_{0II}^2 + 0.002R_{II}^2 - 0.0007\varphi_{PII}^2, \quad (15)$$

series CA - carbon yarn H-30 with thickness 30 tex

$$P_{II} = 2.17 + 1.09P_{0II} - 1.18R_{II} + 0.007\varphi_{PII} + \\ +0.005P_{0II}R_{II} + 0.002P_{0II}\varphi_{PII} - 0.0005R_{II}\varphi_{PII} - \\ -0.0013P_{0II}^2 + 0.07R_{II}^2 - 0.00004\varphi_{PII}^2. \quad (16)$$

For nominal value of the contact angle $\varphi_{PII} = 45°$ in the center of experiment, using dependencies (14-16), Figure 6 represents response surfaces for the II area.

For the III area:

series PA - para-aramid multifilament yarn 44 tex

$$P_{III} = 10.39 + 1.33P_{0III} - 23.88R_{III} + 0.05\varphi_{PIII} - \\ -0.17P_{0III}R_{III} + 0.003P_{0III}\varphi_{PIII} - 0.04R_{III}\varphi_{PIII} - \\ -0.0002P_{0III}^2 + 12.13R_{III}^2 - 0.00003\varphi_{PIII}^2, \quad (17)$$

series MA - meta-aramid multifilament yarn 40 tex

$$P_{III} = 5.88 + 1.18P_{0III} - 11.27R_{III} + 0.02\varphi_{PIII} - \\ -0.11P_{0III}R_{III} + 0.002P_{0III}\varphi_{PIII} - 0.02R_{III}\varphi_{PIII} - \\ -0.00015P_{0III}^2 + 5.69R_{III}^2 - 0.00001\varphi_{PIII}^2, \quad (18)$$

series CA - carbon yarn H-30 with thickness 30 tex

$$P_{III} = 6.84 + 1.20P_{0III} - 13.64R_{III} + 0.25\varphi_{PIII} - \\ -0.12P_{0III}R_{III} + 0.003P_{0III}\varphi_{PIII} - 0.026R_{III}\varphi_{PIII} - \\ -0.00019P_{0III}^2 + 7.00R_{III}^2 - 0.00002\varphi_{PIII}^2. \quad (19)$$

For nominal value of the contact angle $\varphi_{PIII} = 22°$ in the center of experiment, using dependencies (17-19), Figure 7 represents response surfaces for the III area.

Adequacy of obtained regression dependencies has been verified with SPSS program for statistical processing of experimental data [8-14].

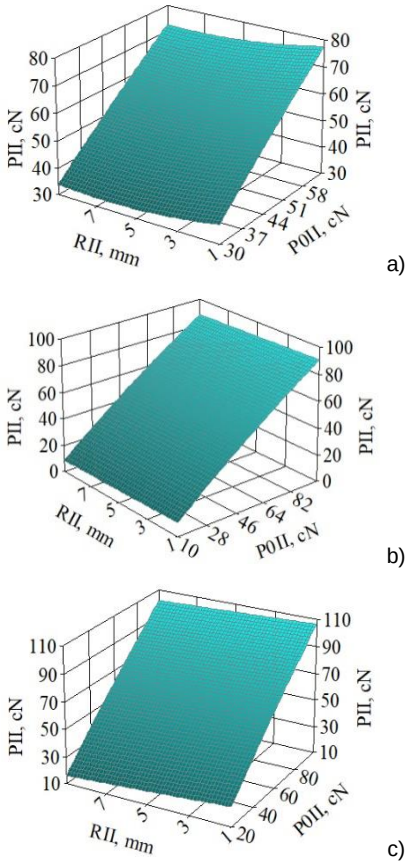

Figure 6 Graphical dependencies of the warp yarns tension for the II area of the weaving loom: a) - para-aramid multifilament yarn; b) - meta-aramid multifilament yarn; c) - carbon yarn H-30

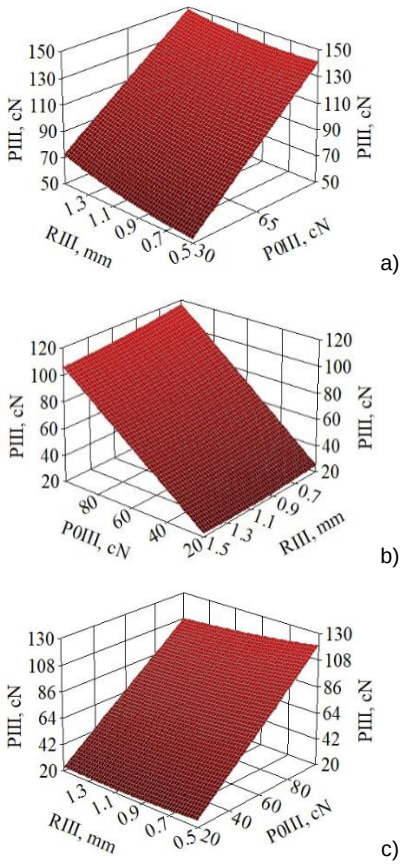

Figure 7 Graphical dependencies of the warp yarns tension for the III area of the weaving loom: a) - para-aramid multifilament yarn; b) - meta-aramid multifilament yarn; c) - carbon yarn H-30

It is of interest to obtain dependency of para-aramid, meta-aramid, and carbon multifilament yarn tension and radius of cylinder with fixed value of input tension. This value of tension corresponds to the center of the experiment (Tables 1-3) for each type of yarn.

Regression dependencies (11-13) for the I area rearranges as follows:

series PA - para-aramid multifilament yarn 44 tex (tension in the center of the experiment 38 cN)

$$P_I = 50.22 - 0.006R_I - 0.00002R_I^2, \quad (20)$$

series MA - meta-aramid multifilament yarn 40 tex (tension in the center of the experiment 26 cN)

$$P_I = 31.67 + 0.0028R_I - 0.00008R_I^2, \quad (21)$$

series CA - carbon yarn H-30 with thickness 30 tex (tension in the center of the experiment 32 cN)

$$P_I = 40.32 + 0.0063R_I - 0.00002R_I^2, \quad (22)$$

Regression dependencies (14-16) for the II area rearranges as follows:

series PA - para-aramid multifilament yarn 44 tex (tension in the center of the experiment 48 cN)

$$P_{II} = 60.27 - 1.17R_{II} + 0.12R_{II}^2, \quad (23)$$

series MA - meta-aramid multifilament yarn 40 tex (tension in the center of the experiment 34 cN)

$$P_{II} = 34.29 - 0.26R_{II} + 0.002R_{II}^2, \quad (24)$$

series CA - carbon yarn H-30 with thickness 30 tex (tension in the center of the experiment 40 cN)

$$P_{II} = 47.36 - 0.99R_{II} + 0.07R_{II}^2, \quad (25)$$

Regression dependencies (17-19) for the III area rearranges as follows:

series PA - para-aramid multifilament yarn 44 tex (tension in the center of the experiment 56 cN)

$$P_{III} = 88.29 - 34.57R_{III} + 12.13R_{III}^2, \quad (26)$$

series MA meta-aramid multifilament yarn 40 tex (tension in the center of the experiment 42 cN)

$$P_{III} = 57.42 - 16.24R_{III} + 5.69R_{III}^2, \quad (27)$$

series CA carbon yarn H-30 with thickness 30 tex (tension in the center of the experiment 48 cN)

$$P_{III} = 67.19 - 19.97R_{III} + 7.00R_{III}^2. \quad (28)$$

Figure 8 represents graphical dependencies reflecting influence of guide's radius on para-amid, meta-aramid, and carbon multifilament yarns tension for the I area, that have been obtained with the use of dependencies (20-22).

Figure 9 represents graphical dependencies reflecting influence of guide's radius on para-amid, meta-aramid, and carbon multifilament yarns tension for the II area, that have been obtained with the use of dependencies (23-25).

Figure 10 represents graphical dependencies reflecting influence of guide's radius on para-amid, meta-aramid, and carbon multifilament yarns tension for the III area, that have been obtained with the use of dependencies (26-28).

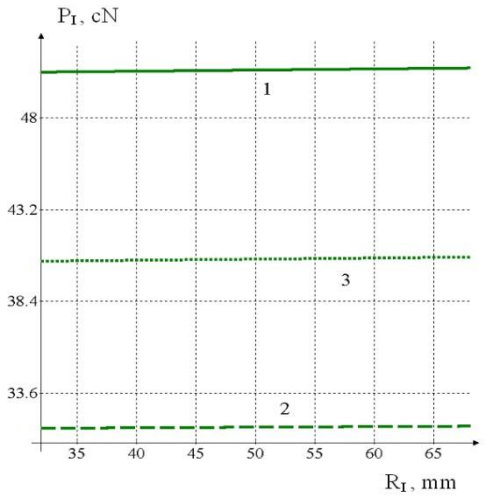

Figure 8 Dependency of para-aramid, meta-aramid, and carbon multifilament yarn tension after the I area: 1 - for series PA; 2 - for series MA; 3 - for series CA

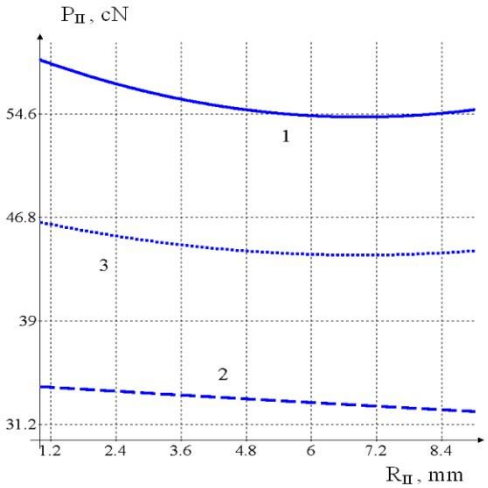

Figure 9 Dependency of para-aramid, meta-aramid, and carbon multifilament yarn tension after the II area: 1 - for series PA; 2 - for series MA; 3 - for series CA

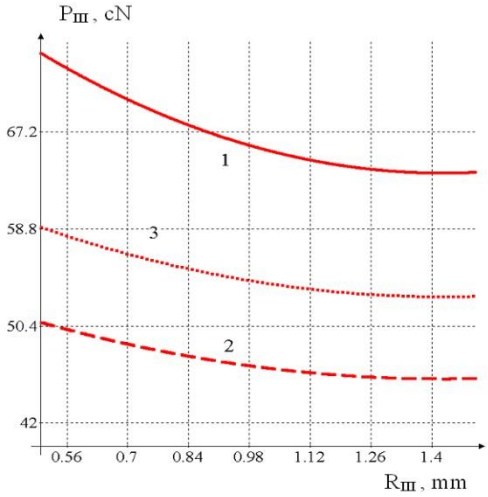

Figure 10 Dependency of para-aramid, meta-aramid, and carbon multifilament yarn tension after the III area: 1 - for series PA; 2 - for series MA; 3 - for series CA

Analysis of the above graphical dependencies allowed to find extreme points with minimum para-aramid, meta-aramid, and carbon multifilament yarns tension for the II, III areas. This permits to bring up a question of optimization of geometrical dimensions of guides and operative parts of the weaving loom.

Using regression dependencies (11-19) we determined values of para-aramid, meta-aramid, and carbon multifilament yarn tension in the III area before the fell of the fabric for different moments of fabric element formation at the weaving looms. The value of distortion of para-aramid, meta-aramid, and carbon multifilament yarns during shedding, as well as during battening and removal of fabric was taken into account as the value of input tension in the I area.

Analysis of graphical dependencies (Figure 11) has allowed to establish that the most dense conditions of fabric formation will be for series PA during manufacturing of Kevlar fabric, where para-aramid multifilament yarns are used as warp yarns 44 tex. This can be explained by the high value of the coefficients of tensile rigidity and bending rigidity.

Obtained results may be used to optimize technological process of weaving, when it will be possible to determine density of the fabric formation process yet during initial stage.

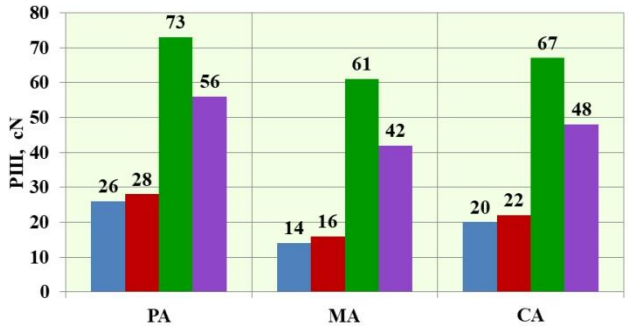

Figure 11 Histogram of warp yarns tension P_{III} before the fell during industrial fabric formation: PA - Kevlar from para-aramid multifilament yarns 44 tex; MA - Nomex from meta-aramid multifilament yarns 40 tex; CA - fabric from carbon multifilament yarns 30 tex; ■ - threading tension of warp yarns; ■ - warp yarns tension working with closed shed; ■ - tension of warp yarns with fully opened shed; ■ - tension of warp yarns during battening

5 CONCLUSIONS

As a result of integrated experimental researches, for para-aramid, meta-aramid, and carbon multifilament yarns were obtained regression dependencies between value of yarn tension after the guide and yarn tension before the guide, radius of guide's surface curve, and contact angle. It has been proven that tension degree of para-aramid, meta-aramid, and carbon multifilament yarns before industrial fabric formation area is influenced by:

1) tension before cylindrical guide surface of the operative part,
2) radius of the cylindrical guide surface curve of the operative part,
3) contact angle between yarns and cylindrical guide surface of the operative part,
4) mechanical, physical and structural properties of para-aramid, meta-aramid, and carbon multifilament yarns.

In the paper three series of experiments has been implemented for the I, II, III threading areas for para-aramid 44 tex, meta-aramid 40 tex and carbon multifilament yarns 30 tex.

The I area corresponded to small curved guide, when the radius of the guide is much longer comparing to the estimated radius of the yarn cross-sectional view. At the same time para-aramid, meta-aramid, and carbon multifilament yarns tension before the guide varies within the limits of $14\ cN \leq P_{0I} \leq 50\ cN$, value of radius of the guide surface curve varies within the limits of $32\ mm \leq R_I \leq 68\ mm$, value of the contact angle between the yarn and guide surface varies within the limits of $98° \leq \varphi_{PI} \leq 122°$.

The II area corresponded to medium curved guide, when the radius of the guide is commensurate with radii of different guides of the weaving looms. At the same time para-aramid, meta-aramid, and carbon multifilament yarns tension before the guide varies within the limits of $17\ cN \leq P_{0II} \leq 63\ cN$, value of radius of the guide surface curve varies within the limits of $1\ mm \leq R_{II} \leq 9\ mm$, value of the contact angle between the yarn and the guide surface varies within the limits of $3° \leq \varphi_{PII} \leq 88°$.

The III area corresponded to large curved guide, when the radius of the guide is commensurate with radii of the para-aramid, meta-aramid, and carbon multifilament yarn cross-sectional view. At the same time para-aramid, meta-aramid, and carbon multifilament yarns tension before the guide varies within the limits of $23\ cN \leq P_{0III} \leq 73\ cN$, value of radius of the guide surface curve varies within the limits of $0.5\ mm \leq R_{III} \leq 1.5\ mm$, value of the contact angle between the yarn and the guide surface varies within the limits of $1° \leq \varphi_{PIII} \leq 44°$.

Due to the above it is now possible, (still at the initial stage of the technological process design) with the use of recursion, to determine para-aramid, meta-aramid, and carbon multifilament yarns tension before the fabric formation area which depends upon geometrical and design parameters of the machinery and its physical and mechanical characteristics.

Obtained results may be used to improve technological processes of the textile industry.

ACKNOWLEDGEMENT: *We are really grateful to the management of Danish Textiles for supporting our experiments with feedstock and providing us with possibility to test results of the investigation in a production environment*

6 REFERENCES

1. Vasconcelos F.B., Marcicano J.P.P., Sanches R.A.: Influence of yarn tension variations before the positive feed on the characteristics of knitted fabrics, Textile Research Journal 85, 2015, pp. 1864-1871, https://doi.org/10.1177/0040517515576327
2. Weber M.O., Ehrmann A.: Necessary modification of the Euler-Eytelwein formula for knitting machines, The Journal of The Textile Institute 103, 2012, pp. 687-690, https://doi.org/10.1080/00405000.2011.598665
3. Koo Y., Kim H.: Friction of cotton yarn in relation to fluff formation on circular knitting machines, Textile Research Journal 72, 2002, pp. 17-20, https://doi.org/10.1177/004051750207200103
4. Shcherban' V., Kolysko O., Melnyk G., Kolysko M., Halavska L., Shcherban' Y.: The influence of the curvature radius of the guiding surface on the tension of polyethylene and polyamide complex yarns during processing on weaving and knitting machines, Vlákna a textil (Fibres and Textiles) 28(3), 2021, pp. 72-81, http://vat.ft.tul.cz/2021/3/VaT_2021_3_8.pdf
5. Shcherban' V., Kolysko O., Melnyk G., Sholudko M., Shcherban' Y., Shchutska G., Kolva N.: Determination of tension for polyamide and basalt multifilament yarns while weaving industrial fabrics, Vlákna a textil (Fibres and Textiles) 28(1), 2021, pp. 75-85, http://vat.ft.tul.cz/2021/1/VaT_2021_1_10.pdf
6. Shcherban' V.Yu.: Determining the technological forces during beating-up in the production of multilayer industrial fabrics, Izvestiya Vysshikh Uchebnykh Zavedenii (Technology of Textile Industry) 3, 1990, pp. 44-47 (in Russian)
7. Vasilchenko V.N., Shcherban' V.Yu.: Effect of the twist of Kapron filament yarn on its bending rigidity, Izvestiya Vysshikh Uchebnykh Zavedenii (Technology of Textile Industry) 4, 1986, pp. 8-9 (in Russian)
8. Shcherban' V., Melnyk G., Sholudko M., Kolysko O., Kalashnyk V.: Improvement of structure and technology of manufacture of multilayer technical fabric, Vlákna a textil (Fibres and Textiles) 26(2), 2019, pp. 54-63, http://vat.ft.tul.cz/2019/2/VaT_2019_2_10.pdf
9. Shcherban' V., Melnyk G., Sholudko M., Kalashnyk V:. Warp yarn tension during fabric formation, Vlákna a textil (Fibres and Textiles) 25(2) 2018, pp. 97-104, http://vat.ft.tul.cz/2018/2/VaT_2018_2_16.pdf
10. Shcherban' V.Yu.: Interaction of stiff yarns with the working parts of knitting and sewing machines, Textile industry 10, 1988, p. 53 (in Russian)
11. Shcherban' V., Melnyk G., Sholudko M., Kolysko O., Kalashnyk V.: Yarn tension while knitting textile fabric, Vlákna a textil (Fibres and Textiles) 25(3), 2018, pp. 74-83, http://vat.ft.tul.cz/2018/3/VaT_2018_3_12.pdf
12. Shcherban' V., Kolysko O., Melnyk G., Sholudko M., Shcherban' Y., Shchutska G.: Determining tension of yarns when interacting with guides and operative parts of textile machinery having the torus form, Vlákna a textil (Fibres and Textiles) 27(4), 2020, pp. 87-95, http://vat.ft.tul.cz/2020/4/VaT_2020_4_12.pdf
13. Shcherban' V., Makarenko J., Melnyk G., Shcherban' Y., Petko A., Kirichenko A.: Effect of the yarn structure on the tension degree when interacting with high-curved guides, Vlákna a textil (Fibres and Textiles) 26(4), 2019, pp. 59-68, http://vat.ft.tul.cz/2019/4/VaT_2019_4_8.pdf
14. Shcherban' V., Makarenko J., Petko A., Melnyk G., Shcherban, Yu., Shchutska G.: Computer implementation of a recursion algorithm for determining the tension of a thread on technological equipment based on the derived mathematical dependences, Eastern-European Journal of Enterprise Technologies 2(1), 2020, pp. 41-50, https://doi.org/ 10.15587/1729-4061.2020.198286
15. Yakubitska Ya I.A., Chugin V.V., Shcherban' V.Yu.: Dynamic analysis of the traversing conditions at the end sections of the groove in a winding drum, Izvestiya Vysshikh Uchebnykh Zavedenii (Technology of Textile Industry) 5, 1997, pp. 33-36 (in Russian), https://ttp.ivgpu.com/?page_id=8140
16. Yakubitskaya I.A., Chugin V.V., Shcherban' V.Yu.: Differential equations for relative yarn movement in the end sections of the channel in the winding drum, Izvestiya Vysshikh Uchebnykh Zavedenii (Technology of Textile Industry) 6, 1997, pp. 50-54 (in Russian), https://ttp.ivgpu.com/?page_id=8195
17. Shcherban' V., Korogod G., Chaban V., Kolysko O., Shcherban' Yu., Shchutska G.: Computer simulation methods of redundant measurements with the nonlinear transformation function, Eastern-European Journal of Enterprise Technologies 2(5), 2019, pp. 16-22, https://doi.org/10.15587/1729-4061.2019.160830
18. Shcherban' V., Korogod G., Kolysko O., Kolysko M., Shcherban' Yu., Shchutska G.: Computer simulation of multiple measurements of logarithmic transformation function by two approaches, Eastern-European Journal of Enterprise Technologies 6(4), 2020, pp. 6-13, https://doi.org/ 10.15587/1729-4061.2020.218517
19. Shcherban' V., Korogod G., Kolysko O., Kolysko M., Shcherban' Yu., Shchutska G.: Computer simulation of logarithmic transformation function to expand the range of high-precision measurements, Eastern-European Journal of Enterprise Technologies 2(9), 2021, pp. 27-36, https://doi.org/ 10.15587/1729-4061.2021.227984
20. Vasilchenko V.N., Shcherban' V.Yu., Apokin Ts.V.: Attachment for holding multilayer fabrics in the clamps of a universal tensile tester, Textile industry 8, 1987, p. 62 (in Russian)
21. Kovar R.: Impact of directions on frictional properties of a knitted fabric, Vlákna a textil (Fibres and Textiles) 14(2), 2007, pp. 15-20, http://vat.ft.tul.cz/Archive/VaT_2007_2.pdf

22. Donmez S., Marmarali A.: A Model for predicting a yarn's knittability, Textile Research Journal 74, 2004, pp. 1049-1054, https://doi.org/10.1177/004051750407401204
23. Liu X., Chen N., Feng X.: Effect of yarn parameters on the knittability of glass ply yam, Fibres & Textiles in Eastern Europe 16(5), 2008, pp. 90-93
24. Hammersley, M.J.: 7-A Simple Yarn-friction Tester for use with knitting yarns, The Journal of the Textile Institute 64(2), 1973, pp. 108-111, https://doi.org/10.1080/00405007308630420
25. Sodomka L., Chrpová E.: Method of determination of Euler friction coefficients of textiles, Vlákna a textil (Fibres and Textiles) 15(2-3), 2008, pp. 28-33, http://vat.ft.tul.cz/Archive/VaT_2008_2_3.pdf